Automated generation of weak formulations

Application to potential-flow simulations on extreme waves arising from soliton interactions

Yang Lu[1] Junho Choi[2] Onno Bokhove[1] Mark A. Kelmanson[1]

Firedrake'23, Missenden Abbey, 15 September 2023

[1]School of Mathematics
University of Leeds, United Kingdom

[2]School of Mathematical Sciences
Korea Advanced Institute of Science and Technology, South Korea

Table of contents

Introduction

- Serious damage and even destruction can be caused by extreme waves.

Introduction

- Serious damage and even destruction can be caused by extreme waves.
- Scale tests are undertaken in wave tanks/basins where such waves are generated using wavemakers.

Introduction

- Serious damage and even destruction can be caused by extreme waves.
- Scale tests are undertaken in wave tanks/basins where such waves are generated using wavemakers.
- Experimental tests $\Leftrightarrow$ Numerical simulations

Variational nonlinear potential-flow model

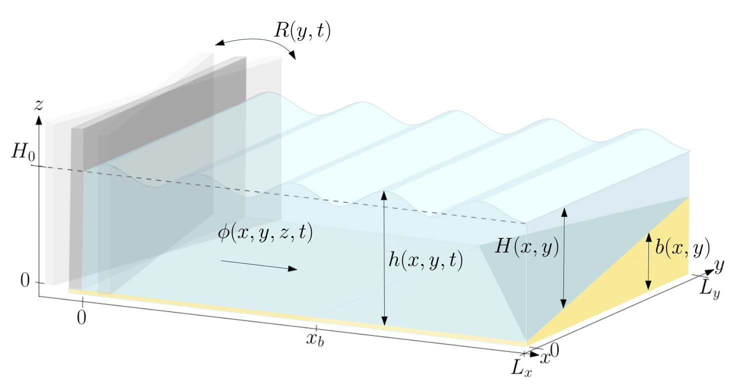

Figure 1: Schematic of the numerical wave tank. Waves are generated by a vertical piston wavemaker oscillating horizontally at $x = R(y,t)$ around $x = 0$. The depth at rest $H(x,y)$ varies in space due to the nonuniform seabed topography $b(x,y)$.

In this study, the nonlinear potential-flow equations (PFE)

$$
\begin{aligned}
\delta\phi:&\ \nabla^2\phi = 0, \quad \text{in } \Omega, && \text{(1a)}\\
(\delta\phi)|_{z=b+h}:&\ \partial_t h + \nabla(h+b)\cdot\nabla\phi - \partial_z\phi = 0, \quad \text{at } z = b+h, && \text{(1b)}\\
\delta h:&\ \partial_t\phi + \frac{1}{2}|\nabla\phi|^2 + g(b+h-H_0) = 0, \quad \text{at } z = b+h, && \text{(1c)}\\
(\delta\phi)|_{x=R}:&\ \partial_x\phi - \partial_y\phi\partial_y R = \partial_t R, \quad \text{at } x = R, && \text{(1d)}
\end{aligned}
$$

are obtained from Luke's variational principle [5]:

$$
0 = \delta\int_0^T\int_{\Omega_{x,y}}\int_{b(x,y)}^{b(x,y)+h(x,y,t)}\left[\partial_t\phi + \frac{1}{2}|\nabla\phi|^2 + g(z-H_0)\right]\mathrm{d}z\,\mathrm{d}x\,\mathrm{d}y\,\mathrm{d}t. \tag{2}
$$

Coordinates transformation

- σ-transformation:

$$x \;\rightarrow\; \hat{x} = \frac{x - \tilde{R}(x,y,t)}{L_w - \tilde{R}(x,y,t)} L_w,$$

$$y \;\rightarrow\; \hat{y} = y,$$

$$z \;\rightarrow\; \hat{z} = \frac{[z - b(x,y)]\, H_0}{h(x,y,t)},$$

$$t \;\rightarrow\; \hat{t} = t.$$

- $\Rightarrow$ **Transformed variational principle (VP)**

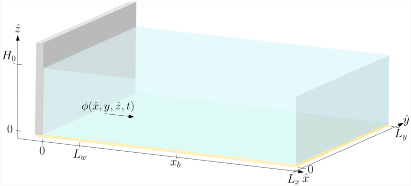

Figure 2: A depiction of the fixed computational domain $\hat{\Omega}$, which is defined as $\hat{\Omega} = \{0 \le \hat{x} \le L_x; 0 \le \hat{y} \le L_y; 0 \le \hat{z} \le H_0\}$.

Numerical model and validation

Numerical discretisation: the “conventional” approach

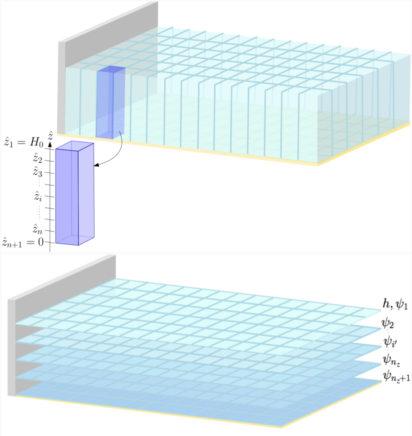

Figure 3: Discretized 3D fixed domain $\hat{\Omega}_d$ [4].

The velocity potential is expanded on the vertical element as

$$\phi(x, y, z, t) = \psi_i(x, y, t)\, \tilde{\varphi}_i(z), \quad (4)$$

where $\tilde{\varphi}_i(z)$ is the Lagrange polynomial.

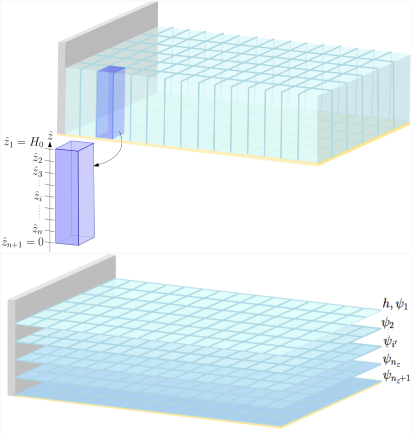

Figure 3: Discretized 3D fixed domain $\hat{\Omega}_d$ [4].

The velocity potential is expanded on the vertical element as

$$\phi(x, y, z, t) = \psi_i(x, y, t)\,\tilde{\varphi}_i(z), \quad (4)$$

where $\tilde{\varphi}_i(z)$ is the Lagrange polynomial.

Unknowns

- $\psi_1(x, y, t)$
- $\hat{\boldsymbol{\psi}}(x, y, t) = [\psi_2, \psi_3, \ldots, \psi_{n_z+1}]^T$
- $h(x, y, t)$

Numerical discretisation: the "conventional" approach

- Substitute expanded ϕ into the transformed VP
  $\Rightarrow$ **Spatial-discritised transformed VP**
- Taking variations with respect to h, ψ_1 and $\hat{\boldsymbol{\psi}}$:

$$\delta h: \quad \int_{\hat{\Omega}_{x,y}} H_0\, \partial_t \left(W\psi_1\right) \delta h \, \mathrm{d}x \, \mathrm{d}y = G\left(h, \psi_1, \hat{\boldsymbol{\psi}}, \tilde{R}\right), \tag{5a}$$

$$\delta \psi_1: \quad \int_{\hat{\Omega}_{x,y}} H_0\, \partial_t h \, \delta(W\psi_1) \, \mathrm{d}x \, \mathrm{d}y = F\left(h, \psi_1, \hat{\boldsymbol{\psi}}, \tilde{R}\right), \tag{5b}$$

$$\delta \hat{\boldsymbol{\psi}}: \quad L\left(h, \psi_1, \hat{\boldsymbol{\psi}}, \tilde{R}\right) = 0. \tag{5c}$$

- Two time-stepping schemes are used, namely first-order **Symplectic-Euler (SE)** and second-order **Störmer-Verlet (SV)**.

Numerical discretisation: the "conventional" approach

- Substitute expanded ϕ into the transformed VP
  $\Rightarrow$ **Spatial-discritised transformed VP**
- Taking variations with respect to h, ψ_1 and $\hat{\boldsymbol{\psi}}$:

$$\delta h: \quad \int_{\hat{\Omega}_{x,y}} H_0\, \partial_t\,(W\psi_1)\,\delta h\,\mathrm{d}x\,\mathrm{d}y = G\left(h, \psi_1, \hat{\boldsymbol{\psi}}, \tilde{R}\right), \tag{5a}$$

$$\delta \psi_1: \quad \int_{\hat{\Omega}_{x,y}} H_0\, \partial_t h\,\delta(W\psi_1)\,\mathrm{d}x\,\mathrm{d}y = F\left(h, \psi_1, \hat{\boldsymbol{\psi}}, \tilde{R}\right), \tag{5b}$$

$$\delta \hat{\boldsymbol{\psi}}: \quad L\left(h, \psi_1, \hat{\boldsymbol{\psi}}, \tilde{R}\right) = 0. \tag{5c}$$

- Two time-stepping schemes are used, namely first-order **Symplectic-Euler (SE)** and second-order **Störmer-Verlet (SV)**.
- Manually-derived explicit weak forms are implemented in *Firedrake*.
- *https://github.com/EAGRE-water-wave-impact-modelling/3D-wave-tank-JCP2022*

Validation against experimental data

The model is also validated against experimental data from a basin test (run number: 202002) conducted at the Maritime Research Institute Netherlands [3].

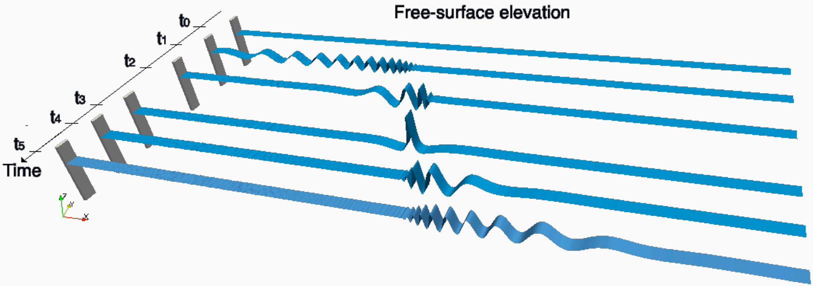

Figure 4: TC4: Temporal snapshots of the free-surface elevation, at times $t_0 = 0.0$s, $t_1 = 93.01$s, $t_2 = 105.12$s, $t_3 = 109.40$s, $t_4 = 113.68$s and $t_5 = 119.98$s. The focussed wave is captured at time $t_3 = 109.40$s, whereafter the wave is defocussing again.

Validation against experimental data

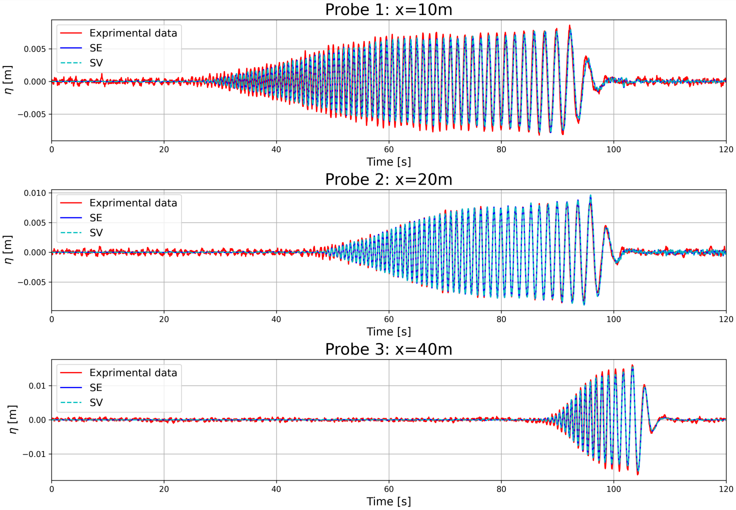

Figure 5: wave elevations of numerical (blue and cyan) and experimental (red) data at the first three probes.

Validation against experimental data

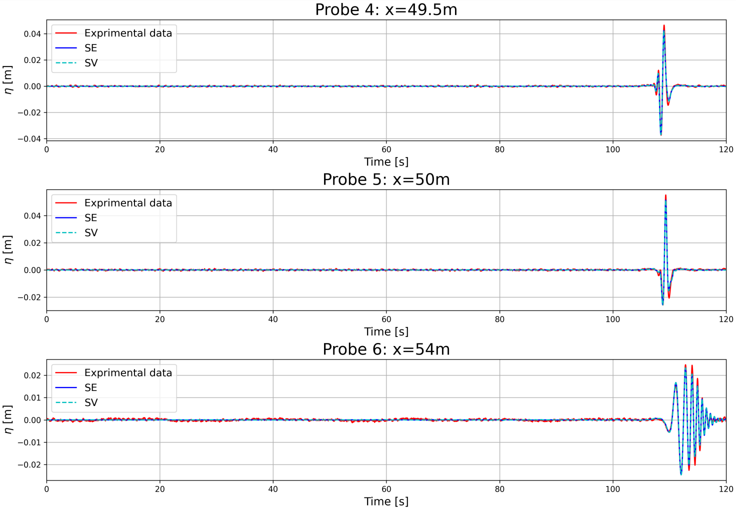

Figure 6: wave elevations of numerical (blue and cyan) and experimental (red) data at the last three probes.

Automated generation of weak formulations

Two-soliton interactions

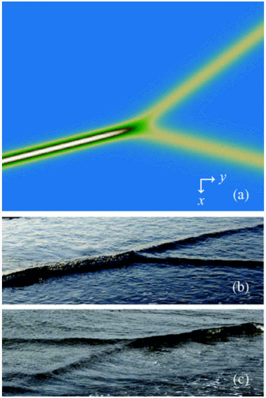

Figure 7: A plot and photographs of a Y-type interaction [1].

Seed the PFE at an initial time with analytical solutions of the *unidirectional* Kadomtsev–Petviashvili equation (KPE).

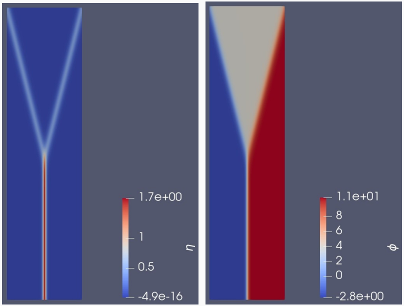

Figure 8: Two-soliton interaction with fourfold amplification achieved ($\eta_{\max} = 4A$)

Numerical model based on the *time-discretised* VP

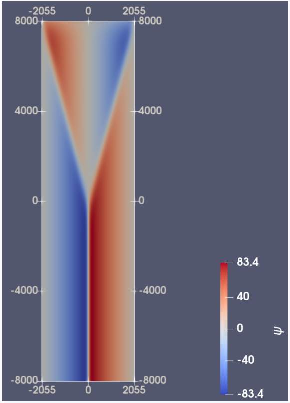

Figure 9: Initial condition for $\tilde{\phi}(x, y, H_0, t_0)$.

- Step 1 Partition the velocity potential

$$\phi(x,y,z,t) = \tilde{\phi}(x,y,z,t) + U_0(y,z)x + c_0(y,z),$$

where U_0 and c_0 can be solved from $\tilde{\phi}(x_1, y, z, t_0) = \tilde{\phi}(x_2, y, z, t_0) = 0$.
Luke's VP $\Rightarrow$ **partitioned VP**

Numerical model based on the *time-discretised* VP

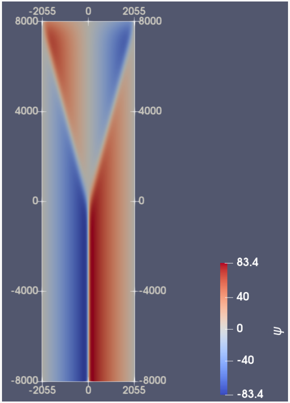

Figure 9: Initial condition for $\tilde{\phi}(x, y, H_0, t_0)$.

- **Step 1** Partition the velocity potential

$$\phi(x, y, z, t) = \tilde{\phi}(x, y, z, t) + U_0(y, z)x + c_0(y, z),$$

where U_0 and c_0 can be solved from $\tilde{\phi}(x_1, y, z, t_0) = \tilde{\phi}(x_2, y, z, t_0) = 0$.
Luke's VP $\Rightarrow$ **partitioned VP**

- **Step 2** σ-transformation
- **Step 3** Free-surface and interior part

$$\tilde{\phi}(x, y, z, t) = \psi(x, y, t)\hat{\phi}(z) + \varphi(x, y, z, t),$$

with $\hat{\phi}(H_0) = 1$ and $\varphi(x, y, H_0, t) = 0$.

Numerical model based on the *time-discretised* VP

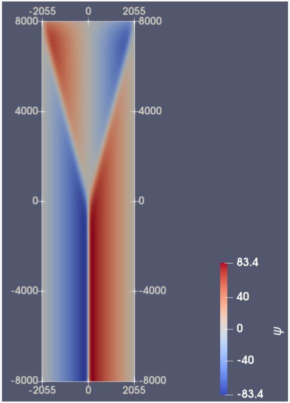

Figure 9: Initial condition for $\tilde{\phi}(x, y, H_0, t_0)$.

- **Step 1** Partition the velocity potential

  $$\phi(x, y, z, t) = \tilde{\phi}(x, y, z, t) + U_0(y, z)x + c_0(y, z),$$

  where U_0 and c_0 can be solved from $\tilde{\phi}(x_1, y, z, t_0) = \tilde{\phi}(x_2, y, z, t_0) = 0$.
  Luke's VP $\Rightarrow$ **partitioned VP**
- **Step 2** σ-transformation
- **Step 3** Free-surface and interior part

  $$\tilde{\phi}(x, y, z, t) = \psi(x, y, t)\hat{\phi}(z) + \varphi(x, y, z, t),$$

  with $\hat{\phi}(H_0) = 1$ and $\varphi(x, y, H_0, t) = 0$.
- **Step 4** Time-discretised VP
  `derivative()`

Time-discretised VP of the modified-midpoint scheme

$$
\begin{aligned}
0 = \delta \iint_{\Omega_h} \int_0^{H_0} & \frac{1}{2}\frac{h^{n+1/2}}{H_0}\Big(U_0 + \hat{\phi}\,\partial_x\psi^{n+1/2} + \partial_x\varphi^{n+1/2} \\
&\qquad\qquad - \frac{z}{h^{n+1/2}}\partial_x h^{n+1/2}\big(\psi^{n+1/2}\,\partial_z\hat{\phi} + \partial_z\varphi^{n+1/2}\big)\Big)^2 \\
&+ \frac{1}{2}\frac{h^{n+1/2}}{H_0}\Big(\partial_y c_0 + x\partial_y U_0 + \hat{\phi}\,\partial_y\psi^{n+1/2} + \partial_y\varphi^{n+1/2} \\
&\qquad - \frac{z}{h^{n+1/2}}\partial_y h^{n+1/2}\big(\partial_z c_0 + x\partial_z U_0 + \psi^{n+1/2}\,\partial_z\hat{\phi} + \partial_z\varphi^{n+1/2}\big)\Big)^2 \\
&+ \frac{1}{2}\frac{H_0}{h^{n+1/2}}\Big(\partial_z c_0 + x\partial_z U_0 + \psi^{n+1/2}\,\partial_z\hat{\phi} + \partial_z\varphi^{n+1/2}\Big)^2\,\mathrm{d}z\,\mathrm{d}x\,\mathrm{d}y \\
+ \iint_{\Omega_h} g h^{n+1/2}\Big(\frac{1}{2}h^{n+1/2} - H_0\Big) &- \psi^{n+1/2}\frac{h^{n+1}-h^n}{\Delta t} + h^{n+1/2}\frac{\psi^{n+1}-\psi^n}{\Delta t}\,\mathrm{d}x\,\mathrm{d}y,
\end{aligned}
\tag{6}
$$

where

$$
\psi^{n+1} = 2\psi^{n+1/2} - \psi^n, \quad h^{n+1} = 2h^{n+1/2} - h^n.
$$

Automated generation of weak forms (1)

```
mesh2d = PeriodicRectangleMesh(..., direction='x', quadrilateral=True)
mesh = ExtrudedMesh(mesh2d, ..., extrusion_type='uniform')

V_W = FunctionSpace(mesh, 'CG', nCG, vfamily='CG', vdegree=nCGvert)
V_R = FunctionSpace(mesh, 'CG', nCG, vfamily='R', vdegree=0)

mixed_Vmp = V_R * V_R * V_W
results_mp = Function(mixed_Vmp)
vvmp = TestFunction(mixed_Vmp)
vvmp0, vvmp1, vvmp2 = split(vvmp)
psimp, hmp, varphimp= split(results_mp)

VP = (...) * ds_t(degree=vpoly) + (...) * dx(degree=vpoly)

# solve h^(n+1/2) wrt psi^(n+1/2)
psif_expr = derivative(VP, psimp, du=vvmp0)
psif_expr = replace(psif_expr, {psi_n1: 2.0*psimp-psi_n0})
psif_expr = replace(psif_expr, {h_n1: 2.0*hmp-h_n0})

h_expr = ...   # solve psi^(n+1/2) wrt hmp=h^(n+1/2)
phi_expr = ... # solve varmp=varphi^(n+1/2)
```

Automated generation of weak forms (2)

```
WF_mp = psif_expr + h_expr + phi_expr
problem_mp = NonlinearVariationalProblem(WF_mp, results_mp, bcs=...)
combo = NonlinearVariationalSolver(problem_mp, solver_parameters=...)

while t <= t_end:
    combo.solve()
    psimp, hmp, varphimp = results_mp.split()

    # n+1 -> n
    h_n0.assign(2.0*hmp - h_n0)
    psi_n0.assign(2.0*psimp - psi_n0)
    phi.interpolate(varphimp + phihat*psi_n0)
```

$\Rightarrow$ Weak forms generated *automatically* and implemented *implicitly*

Potential-Flow simulations on two-soliton interactions

- Basis functions and time resolutions:
  - CG2, (1, 1/2, 1/4) Δt
  - CG4 (Δt, same DoF)
- The new "VP-approach" both shortens the development time and reduces human error.

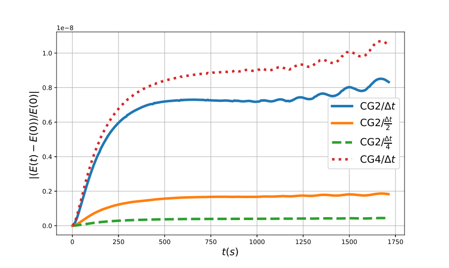

Figure 10: Relative error of energy

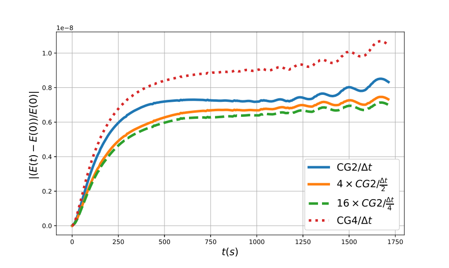

Figure 11: Re-scaled relative error

Potential-Flow simulations on two-soliton interactions

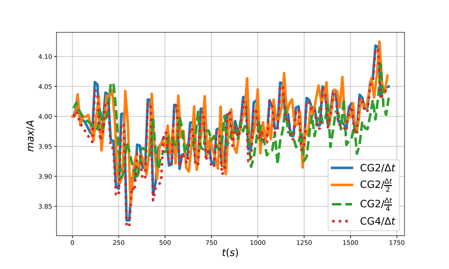

Figure 12: $\eta_{\max}/A$

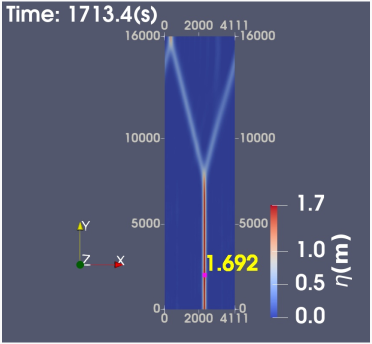

Figure 13: η at $t_{\text{end}} = 1713.4$s

Summary and discussion

Summary and discussion

Summary

In this study, we present a computational tool for simulating 3D nonlinear water waves arising in two contexts:

- high-amplitude waves generated by in-house experimental wavetanks in the maritime industry;
- waves accruing from the interactions of oblique solitons that can occur frequently on flat beaches in nature.

The analysis is based on a fully nonlinear PF water-wave model, and the numerics are conducted through a consistent space-time variational discretisation implemented in *Firedrake*.

Summary and discussion

Summary

In this study, we present a computational tool for simulating 3D nonlinear water waves arising in two contexts:

- high-amplitude waves generated by in-house experimental wavetanks in the maritime industry;
- waves accruing from the interactions of oblique solitons that can occur frequently on flat beaches in nature.

The analysis is based on a fully nonlinear PF water-wave model, and the numerics are conducted through a consistent space-time variational discretisation implemented in *Firedrake*.

Discussion

To address the challenge of wave-breaking, a viscous damping term will be added to the two free-surface BCs locally around the breaking region [2, 6].

Funded by EU Horizon 2020 Marie Curie Actions

Eagre/Aegir: high-seas wave-impact modelling

(project number: 859983)

Thank you!

Questions?

References i

M. J. Ablowitz and D. E. Baldwin.
Nonlinear shallow ocean-wave soliton interactions on flat beaches.
Phys. Rev. E, 86:036305, Sep 2012.

A. Baquet, J. Kim, and Z. Huang.
Numerical modeling using CFD and potential wave theory for three-hour nonlinear irregular wave simulations.
In *Int. Conf. on Offshore Mechanics and Arctic Eng.. In: Offshore Technology*, volume 1, page V001T01A002, 2017.

E. Gagarina, A. Ambati, J. van der Vegt, and O. Bokhove.
Variational space-time (dis)continuous galerkin method for nonlinear free surface water waves.
J. Com. Phys., 275:459–483, 2014.

References ii

F. Gidel.
Variational water-wave models and pyramidal freak waves.
PhD thesis, University of Leeds, 2018.

J. C. Luke.
A variational principle for a fluid with a free surface.
J. Fluid Mech., 27:395–397, 1967.

W. Wang, C. Pakozdi, A. Kamath, and H. Bihs.
A fully nonlinear potential flow wave modelling procedure for simulations of offshore sea states with various wave breaking scenarios.
Applied Ocean Res., 117:102898, 2021.